J. Phys. B: At. Mol. Opt. Phys. **33** (2000) 2859–2867. Printed in the UK PII: S0953-4075(00)50513-6

Comparison of argon and helium (e, 2e) differential cross sections at 64.6 eV using symmetric detection energies and angles

A J Murray, N J Bowring and F H Read

Quantum Dynamics Group, Schuster Laboratory, Manchester University, Manchester M13 9PL, UK

Received 10 April 2000

Abstract. Symmetric (e, 2e) differential cross section measurements for argon at an incident energy of 64.6 eV are presented from the coplanar to the perpendicular plane geometry. The outgoing electrons were detected at symmetric scattering angles and with the same energy. These measurements are compared with analogous results at the same incident energy using helium as the target. The argon (e, 2e) cross section shows a rich and complex structure as the scattering geometry changes, while the very deep interference minimum found in helium is missing.

1. Introduction

The experimental study of the ionization of atoms by electron impact provides a rich source of information for quantum mechanical models of the scattering process. The measurement of angular correlations between scattered and ejected electrons following ionization provides the greatest detail, since the kinematics of the reaction are well defined. These (e, 2e) experiments measure the ionization differential cross section as a function of the momenta of the incident and outgoing electrons involved in the reaction. Theoretical predictions of the reaction can then be compared with the experimental results. At high incident energies distorted-wave and second-order Born calculations now provide accurate agreement with experiment (McCarthy and Weigold 1995, Whelan *et al* 1993). Very close to threshold quantum mechanical forms of the Wannier model (Wannier 1953, Read 1985, Selles *et al* 1987) also prove to be accurate, although the extent of their validity above threshold remains open to question.

It is important to understand ionization in the regime between these extremes, since it is here that most of the ionization processes used in industry and in many natural phenomena occur. In this intermediate energy region, experimental results show that complex variations in the ionization cross section occur for even the simplest of targets (see, for example, Murray and Read 1992, 1993a, b, Röder *et al* 1996, Whelan *et al* 1994). Short- and long-range correlations, ingoing and outgoing channel distortions, post-collisional interactions, interference effects between contributing scattering amplitudes, polarization of the target and exchange processes all play significant roles. Theoretical models then become extremely sensitive to the interplay between these different processes. This restricts the validity of many of the approximations which are used in high- or low-energy regimes and which make the calculations more tractable. Experimental data in the intermediate energy region are therefore not only of fundamental

0953-4075/00/152859+09$30.00

and practical importance, but also provide results which allow new ionization models to be developed.

Most experiments carried out in this energy regime have used helium as a target, since this is the simplest atom which can be easily studied experimentally. Ionization from the $1s^2\,{}^1S_0$ ground state removes an s-electron which has a bound state momentum probability distribution centred around zero, with the most probable momentum of the bound electron being zero. In contrast, ionization of a valence electron from the $(1s^2 2s^2 2p^6 3s^2)3p^6\,{}^1S_0$ ground state of argon removes a p-electron which has a momentum probability distribution that peaks at 0.65 au and has a zero probability for zero momentum (McCarthy and Weigold 1995). Ionization cross section measurements from the valence state of argon are therefore expected to show different characteristics from those of helium due to the difference in the initial state momentum distribution. Furthermore, the effects of the polarization of the target are expected to be more significant in argon than in helium as noted by Rioual *et al* (1997). Similarities between the argon and helium cross sections are also expected, depending upon the interactions that dominate the ionization process. As an example, post-collisional contributions from electron–electron correlations in the outgoing channel are expected to yield similarities in the ionization cross section from both targets.

A further complexity arises due to the different possible ground states of the resulting ion. For helium, the ionic ground state is the $1s\,{}^2S_{1/2}\,He^+$ state 24.58 eV above the neutral ground state. In contrast, the argon ion has two possible ground state configurations depending upon angular momentum couplings between the $3p^5$ valence electrons. The two states are the $3p^5\,{}^2P_{3/2}$ and the $3p^5\,{}^2P_{1/2}$ states located at 15.760 and 15.937 eV, respectively, above the neutral ground state. The (e, 2e) apparatus used in these experiments cannot resolve contributions from these individual ionic states, and so the data presented here are an incoherent mixture of contributions to both final states.

Previous symmetric experiments ionizing argon in this energy regime include those of Bell *et al* (1995) and Rioual *et al* (1997) who both studied coplanar symmetric ionization. Bell *et al* (1995) used an impact energy of 115.8 eV, whereas Rioual *et al* (1997) used impact energies of 115.8, 85.8 and 50 eV. The results presented in this paper are for an impact energy of 64.6 eV, and so can be qualitatively compared with these results. In contrast to these previous studies, the new results use geometries ranging from the coplanar geometry to the perpendicular plane geometry, which is defined when the scattered and ejected electrons emerge in a plane perpendicular to the incident electron direction.

Previous experiments at Manchester on the ionization of helium (e.g. Murray and Read 1992, 1993a, b) were also conducted from the coplanar geometry to the perpendicular plane geometry at incident energies 10–50 eV above the ionization threshold. In these experiments, and in the experiments on argon presented in this paper, the outgoing electrons were detected with equal energy and equal but opposite scattering angles $\xi_a = \xi_b = \xi$ with respect to the projection of the incident electron trajectory onto the detection plane (figure 1). The incident electron angle ψ was varied from $\psi = 0^\circ$ (coplanar geometry) to $\psi = 90^\circ$ (perpendicular plane geometry). For all incident angles ψ a common point exists when $\xi = 90^\circ$, allowing the data to be normalized over the complete set of results for all angles.

To allow comparison with these helium results, the incident electron energy for the experiments presented in this paper was selected to be 64.6 eV. This impact energy is 40 eV above the ionization threshold of helium, and 48.8 eV above the ionization threshold of argon. This energy was chosen as previous observations in helium have revealed a very deep minimum in the ionization cross section at an incident electron angle $\psi = 67.5^\circ$ (Murray and Read 1993b). This minimum is thought to be due to interference between contributing ionization mechanisms, and it was therefore decided to look for similar effects when ionizing argon.

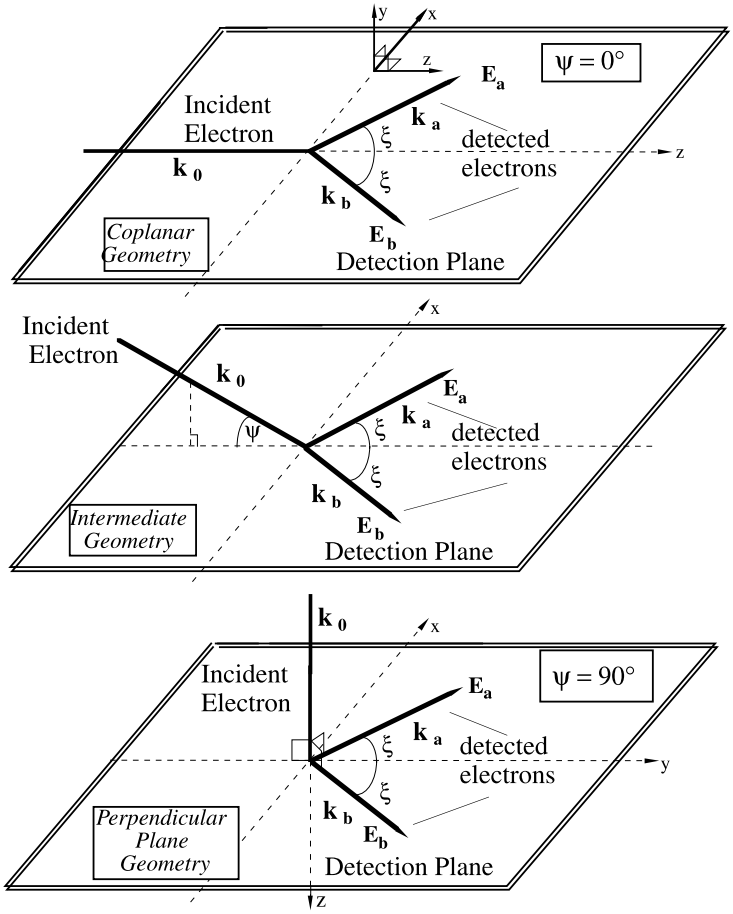

Figure 1. The experimental geometry, showing the evolution from coplanar to perpendicular plane geometry (*a*)–(*c*). The angle ψ is defined as the angle between the detection plane and the direction of the incident electron beam. The scattering angle ξ is defined as the symmetric electron scattering angle in the detection plane.

2. The experimental set-up

The experimental apparatus used to obtain the data is a fully computer-controlled and real-time computer-optimized (e, 2e) spectrometer which has been described elsewhere (Murray *et al* 1992). The computer monitors and controls the spectrometer to maintain optimal operating conditions for the very long data accumulation times required. For experiments on both helium and argon, the vacuum pressure was maintained at 10^{-5} Torr with a residual background pressure of 10^{-8} Torr. The incident electron beam produced in an unselected electron gun had an energy resolution of around 600 meV. The beam was electrostatically focused to a 1 mm diameter beam in the interaction region with a zero beam angle and a pencil angle of 2°. Two hemispherical electron analysers with acceptance half-angles of 3° rotated in the detection plane as defined in figure 1. Coincidences between electrons detected by these analysers then provided angular cross section measurements as the detection angle ξ was varied.

3. Discussion

3.1. Argon

Figure 2 shows the normalized argon ionization data plotted on a logarithmic scale. Nine incident electron directions were selected to provide a comprehensive coverage of the ionization process. These were $\psi = 0^\circ, 7.5^\circ, 15^\circ, 30^\circ, 45^\circ, 60^\circ, 75^\circ, 82.5^\circ$ and 90°. The analyser angular range is restricted by the electron gun and Faraday cup to between $\xi = 35^\circ$ and 125° for $\psi = 0^\circ$–60°, whereas for $\psi > 60^\circ$ it extends from $\xi = 30^\circ$ to 150°.

As noted above, a common point exists for all incident electron directions when $\xi = 90^\circ$. Unfortunately, as can be seen from figure 2, this is close to the minimum in the cross section in argon for all angles ψ. Therefore, in order to allow the results to be adequately normalized, an extensive set of runs was conducted at detection angles $\xi = 40^\circ$ (where the cross section is high and the associated uncertainty is therefore low) and $\xi = 90^\circ$ (where the cross section is low and the associated uncertainty is therefore high) for each angle ψ. By measuring the ionization cross section at these two detection angles continuously over a period of 2 months, an accurate ratio between these measurements was determined, as shown in table 1. The complete set of angular runs was then normalized by setting the measured cross section at $\xi = 40^\circ$ to this ratio.

Table 1. Normalization ratios for the data at different incident angles ψ.

Gun angle ψ	$DCS_{40^\circ}/DCS_{90^\circ}$	Gun angle ψ	$DCS_{40^\circ}/DCS_{90^\circ}$	Gun angle ψ	$DCS_{40^\circ}/DCS_{90^\circ}$
0°	29.7 ± 1.9	30°	24.2 ± 1.7	75°	3.20 ± 0.14
7.5°	46.4 ± 2.4	45°	15.7 ± 0.9	82.5°	4.04 ± 0.23
15°	45.5 ± 2.5	60°	4.94 ± 0.21	90°	4.78 ± 0.17

The results presented in figure 2 show complex variations as the geometry changes from the coplanar geometry to the perpendicular plane geometry. For all geometries the cross section must be zero at detection angles $\xi = 0^\circ$ and 180° due to the Coulomb repulsion between equal energy electrons emerging from the reaction. Hence for $\psi = 0^\circ, 7.5^\circ, 75^\circ$ and 82.5° the low-angle peak must turn over at an angle $\xi < 35^\circ$. Furthermore, for $\psi = 0^\circ$–60°, the peak in the backward-scattering direction ($\xi > 90^\circ$) must also turn over to zero at $\xi = 180^\circ$. It is not possible to ascertain the maximum in the peak heights for these angles.

The observations between $\psi = 0^\circ$ and 45° show a similar trend, with a forward-scattering peak dominating the backscatter peak. Of interest is the evolution of a local minimum observed in the forward coplanar peak at $\xi \simeq 50^\circ$. This dip is characteristic of ionization from a bound p-electron, and is strikingly observed in higher-energy coplanar (e, 2e) measurements (Lahmam-Bennani *et al* 1983, Avaldi *et al* 1988). At high impact energies the dip can be explained using the impulse approximation (McCarthy and Weigold 1995), which assumes that at the point of impact the ion-recoil momentum is equal but opposite to the bound electron momentum $\boldsymbol{q}_e$. In this approximation for symmetric experiments the magnitude of $\boldsymbol{q}_e$ is given by

$$q_e = \left[\{2k_s \cos\xi - k_0 \cos\psi\}^2 + (k_0 \sin\psi)^2\right]^{1/2} \tag{1}$$

where k_0 is the magnitude of the incident electron momentum and k_s is the magnitude of the scattered and ejected electron momenta.

In the experiment described here, the incident electron energy is 64.6 eV and the detection energy of the scattered and ejected electrons is 24.4 eV. Allowing for the ionization energy of

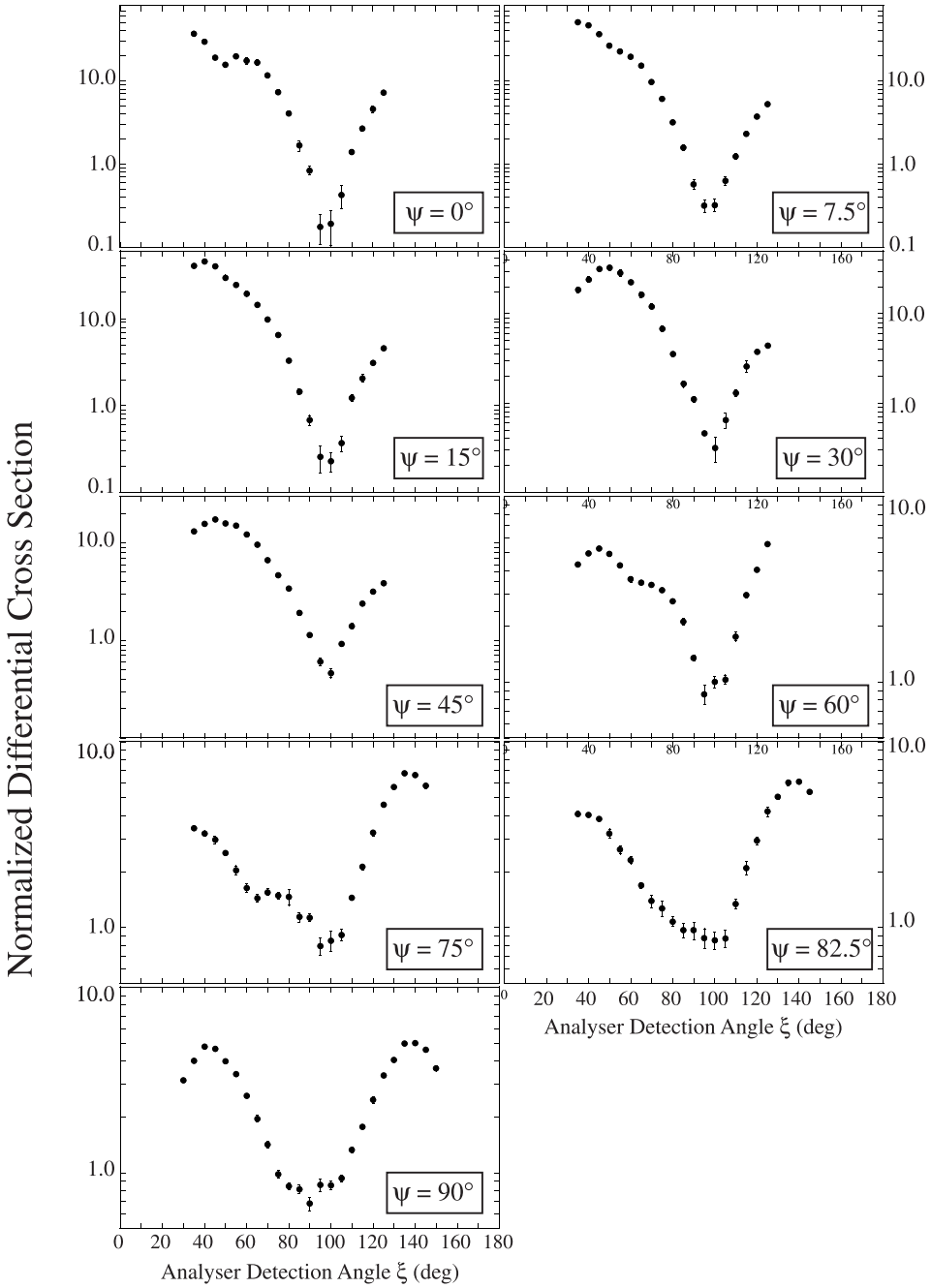

Figure 2. Ionization differential cross sections for argon at 64.6 eV incident energy on a logarithmic scale. The incident electron beam angle was varied over nine selected angles from the coplanar geometry ($\psi = 0°$) to the perpendicular plane geometry ($\psi = 90°$). The results are normalized as detailed in the text.

the bound electron, the magnitudes of the associated momenta for the impact process are then given by $k_0 = 2.18$ au and $k_s = 1.54$ au.

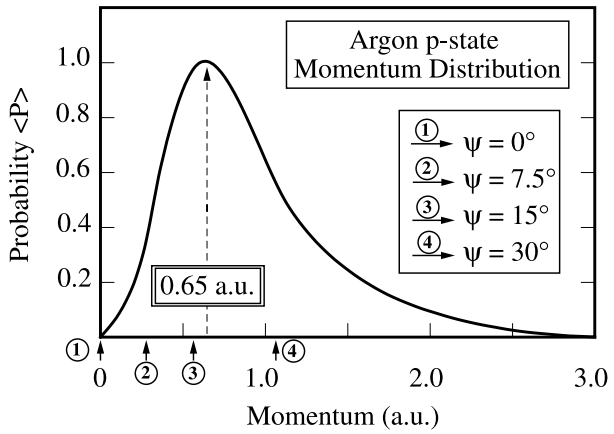

Figure 3. Representation of the bound state electron momentum distribution for the valence shell of argon. The distribution peaks at $q_e = 0.65$ au and is zero for $q_e = 0$. The minimum value of q_e is shown for different incident angles ψ as discussed in the text.

The momentum distribution for the bound p-state valence electron in argon is shown for reference in figure 3. As mentioned above, the momentum distribution peaks at $q_e = 0.65$ au, and is zero when $q_e = 0$. Using equation (1), for the coplanar geometry ($\psi = 0^\circ$) it is possible to find a detection angle ξ for which $\boldsymbol{q}_e$ is equal to zero, and a minimum in the cross section is expected at this angle. In fact, equation (1) gives $\xi = 45^\circ$ when $\psi = 0^\circ$.

For non-coplanar incident angles, a component $k_0 \sin\psi$ of the incident electron momentum always exists orthogonal to the detection plane and so $\boldsymbol{q}_e$ cannot be zero. The smallest possible value of q_e is $k_0 \sin\psi$, which occurs at a detection angle $\xi = \cos^{-1}\frac{k_0 \cos\psi}{2k_s}$.

This minimum value of q_e is shown in figure 3 as a function of the angle ψ. As ψ increases from $\psi = 0^\circ$ (coplanar geometry), the dip in the cross section is therefore expected to fill out until at angles $\psi > \sin^{-1}\frac{0.65 \text{ au}}{k_0}$ (i.e. at $\psi > 17^\circ$) it is no longer possible to calculate an appropriate detection angle ξ for which the dip can be found, since at this angle $q_e^{\min} > 0.65$ au.

This simple analysis is broadly confirmed in the observations shown in figure 2. For the coplanar geometry the dip does not occur at $\xi \simeq 45^\circ$, but is closer to $\xi \simeq 50^\circ$. This is in agreement with the observations of Bell *et al* (1995) and Rioual *et al* (1997). This increase in the angle of the dip may be due to post-collisional interactions between the electrons as they emerge with equal energy from the reaction. Other effects must also be considered since at this energy the impulse approximation is not expected to be accurate when modelling the interaction.

As the incident angle ψ increases to 7.5°, the dip is much less pronounced, and has moved to $\xi \simeq 55^\circ$. The analysis above predicts $\xi = 45.5^\circ$ at this incident angle. When $\psi = 15^\circ$ the dip has almost disappeared, and at $\psi = 30^\circ$ no evidence remains of this effect. It should also be noted that the measured maximum in the cross section at $\xi = 40^\circ$ is larger for $\psi = 7.5^\circ$ and 15° than for the coplanar geometry, as noted in table 1.

As the incident angle is raised to $\psi = 60^\circ$, a new dip appears in the cross section at a detection angle $\xi \simeq 60^\circ$. This dip can also be seen at $\psi = 75^\circ$, but has disappeared when $\psi = 82.5^\circ$. The values of ψ and ξ at which the dip occurs are within 10° of those of a minimum observed in helium, which becomes very deep at $\psi = 67.5^\circ$, $\xi = 70^\circ$ (see figure 4). The dip in argon could therefore be analogous to that in helium, which has been tentatively

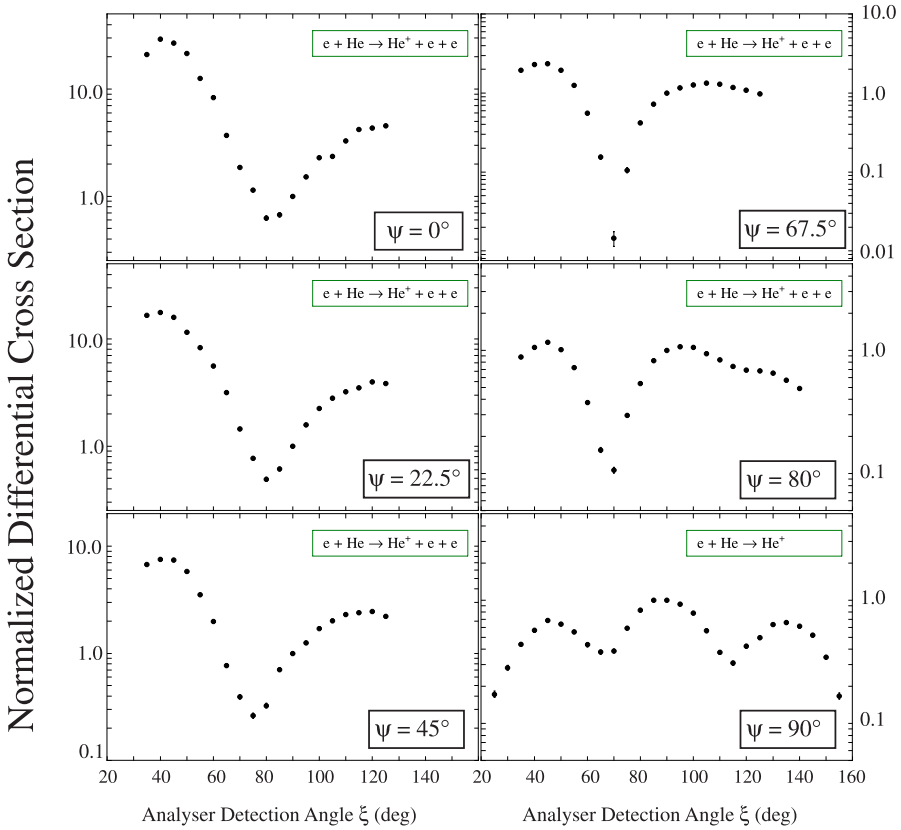

Figure 4. Ionization differential cross sections for helium at 64.6 eV incident energy shown on a logarithmic scale. The incident electron beam angle was varied over six selected angles from coplanar geometry ($\psi = 0^\circ$) to the perpendicular plane geometry ($\psi = 90^\circ$). The results are normalized to unity at the common point $\xi = 90^\circ$.

explained as being due to interference involving a second-order scattering process in which a binary collision of the incident electron with a target electron is followed by the scattering of one of the outgoing electrons in the field of the ion (Bowring *et al* 1999).

An alternative explanation of this dip is that a double-scattering mechanism is occurring in which the incident electron is initially scattered elastically into the detection plane, followed by an ionization reaction in the plane as described by the impulse model above. Although this type of scattering is less probable since the incident energy is higher, it may still provide a significant contribution to the cross section which is observed.

The backscatter peak at $\xi > 90^\circ$ appears to change only slowly in magnitude for all incident angles from $\psi = 0^\circ$ to 90°. In contrast, the forward-scattering peak appears to increase in magnitude as the incident angle moves from $\psi = 0^\circ$ to 15°. The peak then decreases until at $\psi = 75^\circ$ it reaches a minimum. As ψ increases beyond 75° the forward peak once again increases in magnitude, until at $\psi = 90^\circ$ both forward and backscatter peaks are equal, as required by symmetry.

3.2. Helium

The behaviour of the ionization cross section for argon is very different to that of helium at the same incident energy, which is presented in figure 4 for comparison. Results for six different incident angles are shown: $\psi = 0°$, $22.5°$, $45°$, $67.5°$, $80°$ and $90°$. At lower incident angles up to $\psi = 45°$ the cross sections for argon and helium are similar in shape (apart from the dip in argon which is discussed above), however, the minima between forward and backscatter peaks are observed at different detection angles. The helium forward peak decreases monotonically as ψ increases from $0°$ to $90°$, in contrast to argon where this peak increases, decreases and then increases again. The backscatter peak decreases slowly as ψ increases.

Beyond $\psi = 45°$ the ionization cross section for each target differs markedly. For helium, the deep minimum in the cross section is observed when $\psi = 67.5°$. Only a small minimum is observed for argon, as discussed above. In the perpendicular plane ($\psi = 90°$), helium displays a three-peak structure with maxima at $\xi = 50°$, $90°$ and $130°$, the peaks having almost equal magnitude. In contrast, argon shows only a two-peak structure at $\xi = 40°$ and $140°$, with a minimum at $\xi = 90°$. The mechanisms resulting in ionization of argon and helium are clearly very different at these higher incident angles.

4. Conclusions

The differential ionization cross section for argon has been presented over a wide range of symmetric scattering geometries from the coplanar to the perpendicular plane geometry for an incident electron energy of 64.6 eV. The analysers detected equal energy electrons arising from the reaction, and were set at opposing angles with respect to the projection of the incident electron onto the detection plane. This choice of geometry and energy makes possible a sensitive test of the effects of second- and higher-order processes. As with helium, there are indications that at higher values of ψ, secondary scattering in the field of the ion is an important part of the ionization process. Polarization effects and post-collisional interactions are also expected to play important roles.

These results add to the accumulating volume of experimental data for electron-impact ionization at different energies, different scattering geometries and for different target atoms. As these data accumulate, the demands on theoretical models for this process become more stringent. The richness of these results, together with the contrasts noted when ionizing different targets, indicate that there is much still to be learned about ionization in this important energy regime.

Acknowledgments

We would like to thank the Engineering and Physical Sciences Research Council for providing funding for this work. We would also like to thank the technicians in the electronics and mechanical workshops in the Schuster Laboratory for valued support and the maintenance of the experimental apparatus.

References

Avaldi L, Camilloni R, Fainelli E and Stefani G 1988 *J. Phys. B: At. Mol. Opt. Phys.* **21** L359
Bell S, Gibson C T and Lohmann B 1995 *Phys. Rev.* A **51** 2623
Bowring N J, Read F H and Murray A J 1999 *J. Phys. B: At. Mol. Opt. Phys.* **32** L57
Lahmam-Bennani A, Wellenstein H F, Duguet A and Rouault M 1983 *J. Phys. B: At. Mol. Phys.* **16** 121
McCarthy I E and Weigold E 1995 *Electron–Atom Collisions* (Cambridge: Cambridge University Press)

Murray A J and Read F H 1993a *Phys. Rev.* A **47** 3724
——1993b *J. Phys. B: At. Mol. Opt. Phys.* **26** L359
——1992 *Phys. Rev. Lett.* **69** 2912
Murray A J, Turton B C H and Read F H 1992 *Rev. Sci. Instrum.* **63** 3346
Read F H 1985 *Electron Impact Ionization* ed T D Märk and G H Dunn (Vienna: Springer) p 42
Rioual S, Rouvellou B, Pochat A, Rasch J, Walters H R J, Whelan C T and Allan R J 1997 *J. Phys. B: At. Mol. Opt. Phys.* **30** L475
Röder J, Ehrhardt H, Bray I, Fursa D V and McCarthy I E 1996 *J. Phys. B: At. Mol. Opt. Phys.* **29** 2103
Selles P, Huetz A and Mazeau J 1987 *J. Phys. B: At. Mol. Phys.* **20** 5195
Wannier G H 1953 *Phys. Rev.* **90** 817
Whelan C T, Allan R J, Rasch J, Walters H R J, Zhang X, Röder J, Jung K and Ehrhardt H 1994 *Phys. Rev.* A **50** 4394
Whelan C T, Walters H R J, Allan R J and Zhang X 1993 *(e, 2e) and Related Processes* (Dordrecht: Kluwer) p 1